A Cure for the Sonic Point Glitch

J.-M. MOSCHETTA[a],* and J. GRESSIER[b]

[a]*Ecole Nationale Supérieure de l'Aéronautique et de l'Espace;*
[b]*ONERA, Département Modèles pour l'Aérodynamique et l'Energétique,
31055 Toulouse Cedex 4, France*

Among the various numerical schemes developed since the '80s for the computation of the compressible Euler equations, the vast majority produce in certain cases spurious pressure glitches at sonic points. This flaw is particularly visible in the computation of transonic expansions and leads to unphysical "expansion shocks" when the flow undergoes rapid change of direction.

The analysis of this flaw is presented, based on a series of numerical experiments. For Flux-Vector Splitting methods, it is suggested that it is not the order of differentiability of the numerical flux which is crucial but the way the pressure at an interface is calculated. A new way of evaluating the pressure at the interface is proposed, based upon kinetic theory, and is applied to most current available algorithms including Flux-Vector Splitting and Flux-Difference Splitting methods as well as recent hybrid schemes (AUSM, HUS).

Keywords: Upwind schemes, compressible flows, kinetic schemes, sonic point glitch

I. INTRODUCTION

It has been common practice for most numerical schemes designers to concentrate on the capability of a given numerical scheme to adequately capture shock waves and contact discontinuities. Indeed, intense shock waves can be challenging to compute because they require a fairly important amount of numerical dissipation. At the same time, contact discontinuities require as little numerical dissipation as possible in order for a given method to predict the actual effects of natural viscosity, not the effects of the numerical viscosity. Recently, many efforts have been made to design numerical schemes that satisfy this double requirement (Liou and Steffen, 1993; Coquel and Liou, 1992; Moschetta and Pullin, 1997). These recent efforts have demonstrated that it is ambiguous to speak about the "dissipation" of a given numerical scheme without specifying in which situation this dissipation becomes active. Numerical dissipation is a twofold concept in which the "good" dissipation allows to capture shock waves and nonlinear phenomena in general, and the "bad" dissipation

---

*Corresponding author.

artificially broadens boundary layers and requires high level of grid resolution.

However, few authors have considered to assess the capability of numerical schemes to correctly compute expansion waves. Sod's problems, which belong to the very first test cases which one is usually advised to start with, include a traveling shock wave, an expansion fan and a contact discontinuity. In the supersonic Sod problem, the expansion fan contains a sonic point where virtually all numerical schemes produce an unphysical glitch. Even such elaborate schemes as Osher scheme, or Godunov scheme produce the same kind of glitch in the vicinity of the sonic point. To the best of the authors' knowledge, the only schemes which do not seem to be affected by this flaw are kinetic schemes (or Boltzmann schemes) such as EFM (Pullin, 1980), EFMO (Moschetta and Pullin, 1997) or BGK (Xu *et al.*, 1995), and the recent box-scheme proposed by Chattot (Chattot, 1998). The sonic point glitch problem is not limited to the supersonic 1D Sod problem but is closely related to the spurious focusing of pressure contours when the flow gets round a corner in the case of an irregular 2D body shape. It is therefore important to get rid of this flaw particularly when irregular shapes are considered.

This paper addresses some of the mathematical questions which underlie the sonic point glitch problem, with a particular focus on a simple modification which contributes to cure the flaw for a large number of current available shock-capturing schemes. The proposed modification reproduces some of the mathematical properties satisfied by kinetic schemes that seem to be decisive for the problem considered and does not affect the capability of a numerical method to exactly capture contact discontinuities.

2. ANALYSIS

Consider the discretization of the 1D Euler equations

$$\frac{\partial U}{\partial t} + \frac{\partial F}{\partial x} = 0 \qquad (1)$$

where $U = (\rho, \rho u, \rho E)^T$ is the state vector of conservative variables, $F = (\rho u, \rho u^2 + p, \rho u H)^T$ is the Euler flux and H is the total enthalpy defined as $H = E + p/\rho$. Consider the following family of Flux-Vector Splitting (FVS) schemes: Steger–Warming (Steger and Warming, 1981); Van Leer (Van Leer, 1982) and EFM (Pullin, 1980). All three schemes are FVS schemes in the sense that their numerical flux function can be expressed as

$$F(U_L, U_R) = F^+(U_L) + F^-(U_R) \qquad (2)$$

where U_L and U_R are the left and right state vectors respectively. Although based on fairly different mathematical or physical approaches, the three corresponding numerical fluxes can all be expressed as

$$F(U_L, U_R) = \mathcal{M}_L^+(a\Phi)_L + \mathcal{M}_R^-(a\Phi)_R + \mathcal{P}_L^+ \cdot P_L + \mathcal{P}_R^- \cdot P_R \qquad (3)$$

where

$$\Phi = \begin{pmatrix} \rho \\ \rho u \\ \rho H \end{pmatrix}, \quad P = \begin{pmatrix} 0 \\ p \\ 0 \end{pmatrix} \qquad (4)$$

In the above expression, $\mathcal{M}^\pm$ and $\mathcal{P}^\pm$ are scalar functions of the local Mach number M, based on the velocity component normal to the interface, and a is the local sound speed. Actually, all FVS methods presented above have been modified according to the suggestion of Hänel (Hänel, 1987) so that the energy flux has the following form:

$$F_{\text{energy}}^\pm = F_{\text{mass}}^\pm \cdot H \qquad (5)$$

in order for a stationary inviscid solution to ensure constant total enthalpy H throughout the flowfield. Therefore, the three flux functions considered here only differ from one another by the expression of their scalar functions $\mathcal{M}^\pm$ and $\mathcal{P}^\pm$. The pressure function $\mathcal{P}^\pm$ can actually be interpreted as a normalized weight coefficient ranging from 0 to 1 which allows to evaluate the interface pressure from pressure values at either sides of the interface. For the three FVS methods considered here, the following pressure functions are used

Steger – Warming

$$\mathcal{P}_{SW}^{\pm} = \begin{cases} \frac{1}{2}(1 \pm \text{sign}\,(M)) & \text{if } |M| > 1, \\ \pm \frac{1}{2}(M \pm 1) & \text{otherwise.} \end{cases} \quad (6)$$

Van Leer

$$\mathcal{P}_{VL}^{\pm} = \begin{cases} \frac{1}{2}(1 \pm \text{sign}\,(M)) & \text{if } |M| > 1, \\ \pm \frac{1}{4}(M \pm 1)^2 (2 \mp M) & \text{otherwise.} \end{cases} \quad (7)$$

EFM

$$\mathcal{P}_{EFM}^{\pm} = \frac{1}{2}(1 \pm \text{erf}(\alpha M)) \quad (8)$$

where $\alpha = \sqrt{\gamma/2} \simeq 0.84$. The error function erf is defined as

$$\text{erf}(s) = \frac{2}{\sqrt{\pi}} \int_0^s \exp(-t^2) dt \quad (9)$$

The physical interpretation of scalar functions $\mathcal{M}^{\pm}$ is more subtle to establish. First, they have the dimension of a Mach number and consequently are not bounded. Second, in the special case where pressure values are equal on either sides of the interface, such as in the case of a steady contact discontinuity, they account for the averaging of the left and right fluxes. Third, the upwinding mechanism of the method totally relies on their expression and is then of major importance for shock-capturing properties. For the three FVS methods considered here, the Mach number functions $\mathcal{M}^{\pm}$ are defined as

Steger – Warming

$$\mathcal{M}_{SW}^{\pm} = \begin{cases} \frac{1}{2}(M \pm |M|) & \text{if } |M| > 1, \\ \pm \frac{1}{2\gamma}[\gamma M \pm (\gamma - 1)|M| \pm 1] & \text{otherwise.} \end{cases} \quad (10)$$

Van Leer

$$\mathcal{M}_{VL}^{\pm} = \begin{cases} \frac{1}{2}(M \pm |M|) & \text{if } |M| > 1, \\ \pm \frac{1}{4}(M \pm 1)^2 & \text{otherwise.} \end{cases} \quad (11)$$

EFM

$$\mathcal{M}_{EFM}^{\pm} = \frac{1}{2}[1 \pm \text{erf}(\alpha M)]M \pm \frac{1}{2\alpha\sqrt{\pi}}\exp(-\alpha^2 M^2) \quad (12)$$

Close observation of the different expressions for $\mathcal{P}$ and $\mathcal{M}$ reveals that EFM functions differ from the two other FVS methods by two specific properties:

1. EFM functions are infinitely differentiable (C^∞) with respect to the Mach number M while Steger – Warming's and Van Leer's are not infinitely differentiable at $M = \pm 1$ (Steger – Warming functions are only C^0 and Van Leer functions are C^1),
2. EFM functions are not fully upwind in the sense that there is always a relatively small contribution from downstream even if the local Mach number is greater than 1.

The second property results from the fact that EFM is based upon a statistical description of gases in which there is always some probability to find a particle of gas going backward in a supersonic flow. In the following, the expression *fully upwind* will refer to a method in which there is no influence from downstream when the flow is locally supersonic. For a FVS method, this requirement will read

$$F^+(U_L) = F_L, \quad F^-(U_L) = 0, \quad \text{if } M_L > 1$$

$$F^+(U_R) = 0, \quad F^-(U_R) = F_R, \quad \text{if } M_R < -1 \quad (13)$$

where F_L and F_R stand for the exact flux taken at U_L and U_R respectively. Since EFM is the only FVS method that is not affected by the sonic point glitch, it is interesting to identify which of the two cited properties is involved in the sonic point problem. In order to sort this out, a fourth FVS method called *Upwind Infinitely Differentiable* scheme (UID) is constructed in such a way that the functions $\mathcal{P}$ and $\mathcal{M}$, and consequently the numerical flux itself, is infinitely differentiable and fully upwind at the same time. A suitable choice for $\mathcal{P}$ and $\mathcal{M}$ is given below

UID

$$\mathcal{P}_{UID}^{\pm} = \frac{1}{2}[1 \pm \text{erf}(Y)] \quad (14)$$

$$\mathcal{M}_{UID}^{\pm} = \frac{1}{2}[1 \pm \text{erf}(Y)]M \pm \frac{1}{2\alpha\sqrt{\pi}} \exp(-Y^2) \quad (15)$$

with

$$Y = \text{arg tanh}\,(\beta M) \quad (16)$$

The parameter β accounts for the closeness of the functions with respect to their asymptotes. In the present study, $\beta = 3/2$ has been selected. It must be pointed out that the UID functions are C^∞ which means that, like EFM functions, their derivatives of any order are zero in the vicinity of sonic points. However, as opposed to EFM functions, UID functions ensure full upwinding when the local Mach number is greater than 1. Figure 1 shows the different functions $\mathcal{P}$ and $\mathcal{M}$ which completely define the following numerical schemes: Steger–Warming, Van Leer, EFM and UID.

3. NUMERICAL RESULTS

3.1. Test Case (1)

A first series of computations have been carried out on the supersonic 1D Sod's problem which can be defined by the following initial conditions:

$$\begin{aligned} \rho_L &= 1, & p_L &= 10^5, & u_L &= 0 \\ \rho_R &= 0.01, & p_R &= 10^3, & u_R &= 0 \end{aligned} \quad (17)$$

Numerical results can be compared with the analytical solution at $t = 0.03$ before the 0 waves reach the tube ends. Figure 2 shows numerical results obtained with a uniform grid of 100 points using the following methods: Van Leer, UID and EFM. It can be observed that Van Leer and UID results display a clear gap in the vicinity of the sonic point. The sonic point glitch seems to be even more pronounced with UID than with Van Leer showing that smoothness of the numerical flux function does not solve the problem at all. Following the same idea, AUSM scheme (Liou, 1993) is modified using EFM pressure function.

AUSM differs from FVS methods in the sense that the weighting functions $\mathcal{M}^{\pm}$ for the convective fluxes can depend on both states and not only on the state associated with the corresponding convective flux. In other words, referring to Eq. (3), the numerical flux for AUSM can be expressed as:

$$F^{AUSM}(U_L, U_R) = \mathcal{M}_{L/R}^{+}(a\Phi)_L + \mathcal{M}_{L/R}^{-}(a\Phi)_R + \mathcal{P}_L^{+} \cdot P_L + \mathcal{P}_R^{-} \cdot P_R \quad (18)$$

where $\mathcal{M}_{L/R}^{\pm}$ are functions of both left and right states and not functions of just only one state as in regular FVS methods. This idea gives an additional degree of freedom to ensure exact resolution of contact discontinuity. The actual functions $\mathcal{M}_{L/R}^{\pm}$ are defined as

$$\mathcal{M}_{L/R}^{\pm} = 1/2(\mathcal{M}_{L/R} \pm |\mathcal{M}_{L/R}|) \quad (19)$$

with

$$\mathcal{M}_{L/R} = \mathcal{M}_{L}^{+} + \mathcal{M}_{R}^{-} \quad (20)$$

At this point, there is some flexibility in the choice of scalar functions $\mathcal{M}^{\pm}$. In the original AUSM method, Van Leer's functions are used. Obviously, other choices, such as those mentioned in the present paper, are available. In the present study, the original approach using Van Leer's Mach number function has been followed. Only the pressure functions have been modified. Formally, the resulting AUSMK method only differs from the original AUSM method in the way $\mathcal{P}$ is evaluated. Instead of using Van Leer's pressure function, which contains a switch according to the value of $|M|$, AUSMK consists of using EFM pressure function (defined by Eq. (8)) which has a unique expression regardless of the relative position of $|M|$ with respect to 1. It is interesting to observe on Figure 3 that the sonic point glitch associated with the original version of AUSM is perfectly cured by this simple modification. Because it only affects the pressure term in the numerical flux, it does not degrade the ability of AUSM to exactly capture stationary contact
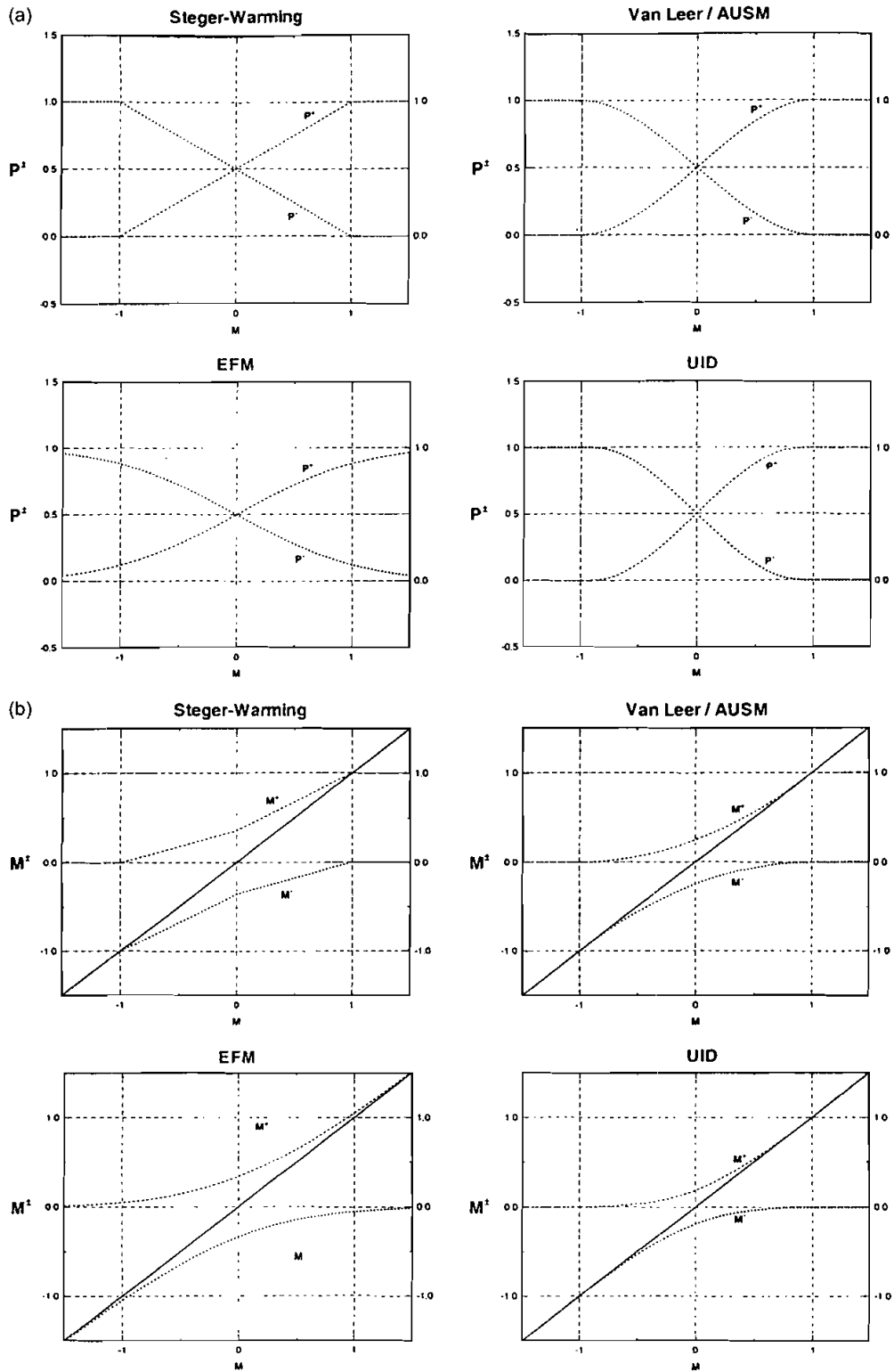
FIGURE 1   (a) Pressure functions and (b) Mach number functions for different algorithms: Steger–Warming, Van Leer or AUSM, EFM and UID.
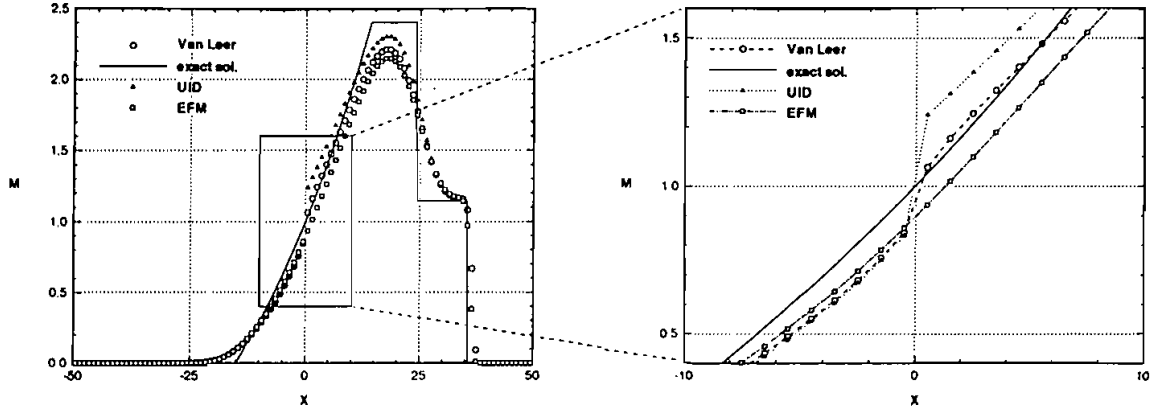
FIGURE 2   Supersonic Sod problem: computed Mach numbers for Van Leer UID and EFM schemes.
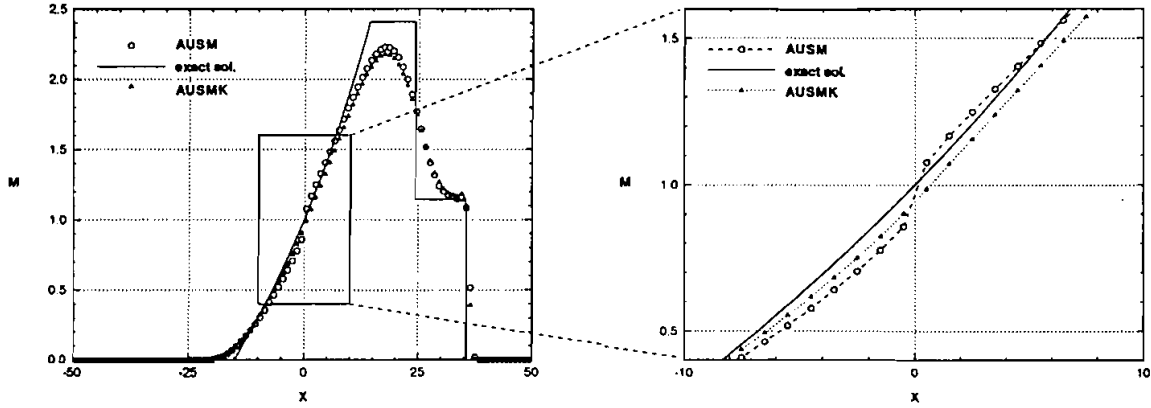

FIGURE 3   Supersonic Sod problem: computed Mach numbers for AUSM and AUSMK schemes.

discontinuities. A similar modification could be applied to the Mach number function but numerical experiments have shown that although the sonic point glitch is also removed, shock waves are then slightly thicker. In the present form, the difference between AUSM and AUSMK consists of the addition to a *kinetic pressure correction* term (KPC) of the following form

$$F^{AUSMK}(U_L, U_R) = F^{AUSM}(U_L, U_R)$$
$$+ \Delta P_L^+ \cdot P_L + \Delta P_R^- \cdot P_R \quad (21)$$

where

$$\Delta P^\pm = P_{EFM}^\pm - P_{VL}^\pm \quad (22)$$

From the previous expression, it is clear that AUSMK reverts to the original formulation of AUSM in the case of the computation of a stationary boundary layer where $M_L = M_R = 0$, thus $\Delta P^\pm = 0$. The proposed correction does not add the "bad" dissipation which would artificially broaden boundary layers. Furthermore, Eq. (21) shows that any flux function can be modified by adding to the original function the KPC term defined by $\Delta P^\pm$. Following this idea, Roe scheme (Roe, 1981), which is known to suffer from a tendency to expansion shocks, is modified by adding the KPC term as follows

$$F^{ROE-K} = F^{ROE} + \Delta F \quad (23)$$

with

$$\Delta F = \Delta \mathcal{P}^+ \cdot P_L + \Delta \mathcal{P}^- \cdot P_R \qquad (24)$$

in which $\Delta \mathcal{P}^\pm$ are defined by Eq. (22). When Roe scheme is modified along these lines, the resulting Roe-K scheme produces no glitch at the sonic point and yet maintains the same capability of exactly resolving contact discontinuities or, equivalently, boundary layers. However, like the entropy fix of Harten, the use of the KPC term does not maintain the exact resolution of steady shock waves. This modified version of Roe scheme has been compared with the usual entropy-fixed version of Roe scheme which consists of replacing the absolute value applied to the wave speeds $u - a$, u, $u + a$ with Harten's function (Harten and Hyman, 1983) defined as:

$$\Psi(\lambda) = \begin{cases} \dfrac{\lambda^2 + \delta^2}{2\delta} & \text{if } |\lambda| < \delta \\[2mm] |\lambda| & \text{otherwise} \end{cases} \qquad (25)$$

where δ is related to the spectral radius of the Euler flux Jacobian matrix as:

$$\delta = \delta_0 \cdot (|u| + a) \qquad (26)$$

On Figure 4, numerical results for the supersonic Sod problem are shown using the original

Roe scheme, the entropy-fixed Roe scheme with $\delta_0 = 0.2$ and the modified Roe-K scheme. It can be observed that the usual entropy fix applied to Roe scheme using a typical value for Harten's parameter does not completely remove the typical glitch at the sonic point as opposed to the present modification which leads to perfect smoothness around the sonic point.

3.2. Test Case (2)

In order to specify the problem encountered in the vicinity of sonic points when computing a transonic expansion, an additional test case is proposed which consists of computing a shock tube problem starting from initial conditions which correspond to a pure transonic expansion fan. The initial conditions are defined as follows:

$$p_L = 1, \quad p_L = 10^5, \quad u_L = 0 \qquad (27)$$

The right state is calculated so that the following relations are satisfied:

$$p_R / \rho_R^\gamma = p_L / \rho_L^\gamma \qquad (28)$$

$$u_R + \frac{2a_R}{\gamma - 1} = u_L + \frac{2a_L}{\gamma - 1} \qquad (29)$$

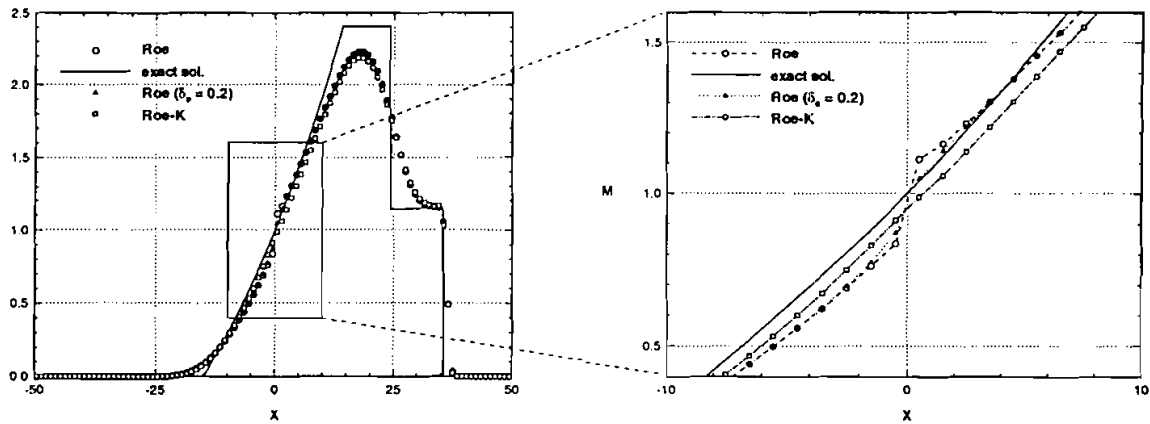$$M_R = u_R / a_R = 2.0 \qquad (30)$$

FIGURE 4   Supersonic Sod problem: computed Mach numbers for Roe, entropy-fixed Roe and Roe-K schemes.

The above relations completely define the right state in such a way that a pure expansion fan develops between the initial interface. Figure 5 shows a series of computations of the expansion fan at time $t = 5.0 \times 10^{-4}$ s in terms of the Mach number distribution magnified around the sonic point region. For this computation, a uniform grid of 200 points is used. Figure 5(a) compares numerical results obtained with Van Leer and Van Leer-K methods respectively. Figure 5(b) compares numerical results obtained with AUSM and AUSMK methods respectively. In both cases, a clear improvement is obtained with regard to the problem considered. Two additional FDS schemes, namely Osher (Osher and Solomon, 1982) and

Godunov (Godunov, 1959) schemes are also modified according to the present modification, giving the corresponding Osher-K and Godunov-K schemes. Numerical results are shown on Figures 5(c) and 5(d). For Osher scheme, the order chosen for the eigenvalues is the natural order but further analysis showed that the original version of Osher's scheme using the inverse order suffers from the same flaw. Actually, both versions can be cured by the present modification. Surprisingly, Godunov scheme which is based on an exact Riemann solver, leads to the same unphysical glitch. It should be pointed out that in the case of a pure expansion fan, the computation of Godunov numerical flux does not require any Newton iterations which
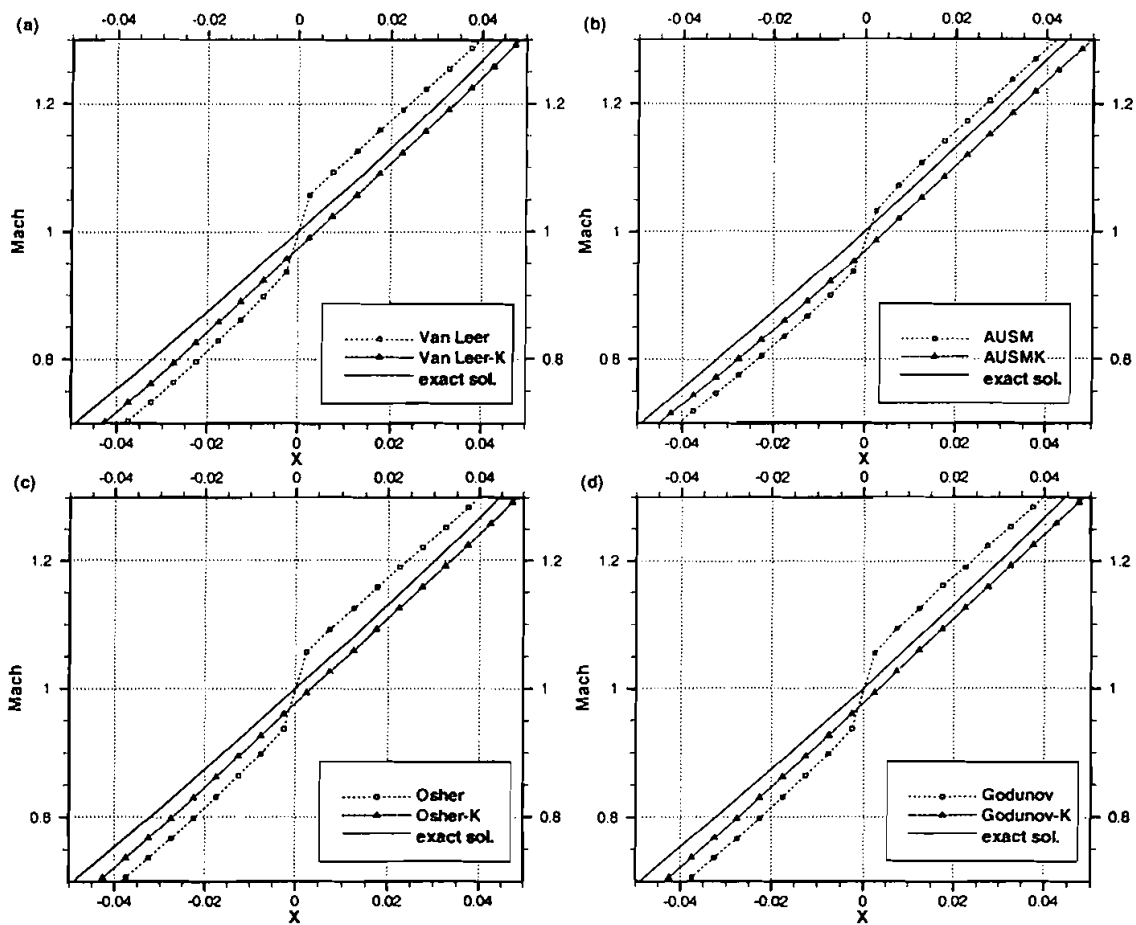

FIGURE 5   Transonic expansion: computed Mach numbers for (a) Van Leer/Van Leer-K, (b) AUSM/AUSMK, (c) Osher/Osher-K and (d) Godunov/Godunov-K.

might have introduced some numerical errors. One explanation for the sonic glitch problem might be that at the interface corresponding to the sonic point, all classical methods, with the exception of kinetic schemes, produce a numerical flux which is only dependent on the left subsonic state. This can be easily checked for FVS methods: since $M_R > 1$, the pressure and Mach number functions $\mathcal{P}_R^-$ and $\mathcal{M}_R^-$ return zero. Hence, the flux at the interface only depends on the left state through the following relation

$$F_{L/R} = \mathcal{M}_L^+(a\Phi)_L + \mathcal{P}_L^+ \cdot P_L \qquad (31)$$

AUSM flux reduces to the same expression since, when $M_R > 1$ and $0 < M_L < 1$

$$\mathcal{M}_{L/R} = \mathcal{M}_L^+,$$
$$\mathcal{M}_{L/R}^+ = \mathcal{M}_L^+, \qquad (32)$$
$$\mathcal{M}_{L/R}^- = 0.$$

Therefore, it will take longer for a fully upwind flux function, such as the regular AUSM method, to let a continuous solution (e.g., an expansion fan) replace an initial discontinuous solution since acoustic waves will remain blocked on the supersonic side of the sonic region.

In the present correction term, one may argue that the use of the error function is not mandatory in principle since the C^∞ property cannot, by itself, remove the sonic point glitch. Therefore, a different way of implementing the partial upwinding mechanism within the numerical flux function has been developed. It simply consists of using Van Leer's pressure function on an extended range as follows. Instead of using $\Delta\mathcal{P}^\pm = \mathcal{P}_{\text{EFM}}^\pm - \mathcal{P}_{\text{VL}}^\pm$ (22), which require the error function, one can simply use:

$$\Delta\mathcal{P}^\pm(M) = \mathcal{P}_{\text{VL}}^\pm(\mu M) - \mathcal{P}_{\text{VL}}^\pm(M) \qquad (33)$$

in which $\mu = 0.9$. This leads to an "extended" Van Leer's pressure correction term which equally ensures the upstream influence in supersonic region (at least where $1 < |M| < 1/\mu$). The kinetic pressure correction term is compared to the

extended Van Leer's pressure correction on Figure 6(a). This comparison indicates that the glitch can be also adequately removed by using Van Leer's extended pressure correction term (33). However, Figure 6(b), on which the gradient of the computed Mach number is plotted, reveals that although Van Leer's extended pressure correction term provides smooth transition through the sonic point, it brings a slight bump immediately downstream the sonic point as opposed to the kinetic pressure correction term.

Using the same test case, two additional calculations have been performed. The first one was aimed at determining whether the sonic point glitch would disappear or not when the grid resolution is increased. On Figure 7(a), three numerical results are compared with the exact solution using 200, 400 and 800 points equally spaced in the computational domain. The gap size is apparently of the order $O(h)$ since it is reduced by a factor of 2 when the number of points is multiplied by two. However, when plotting the gradient of the Mach number (see Fig. 7(b)) one can observe that the peak associated with the sonic glitch does not vanish when the grid resolution is increased. Therefore, resorting to a higher grid resolution is not the clue for solving the problem. The second calculation (see Fig. 8) illustrates that the use of high order methods leads to a drastic reduction in the sonic gap. A standard MUSCL reconstruction applied to the primitive variables $W = (\rho, u, p)^T$ with the minmod limiter and an upwinding parameter $\phi = -1$ has been used to upgrade the original Van Leer's scheme to second order accuracy in space.

$$W_{j+1/2}^L = W_j + \frac{1-\phi}{4}\tilde{\Delta}_{j-1/2} + \frac{1+\phi}{4}\tilde{\Delta}_{j+1/2}$$
$$W_{j+1/2}^R = W_{j+1} - \frac{1+\phi}{4}\tilde{\Delta}_{j+1/2} - \frac{1-\phi}{4}\tilde{\Delta}_{j+3/2} \qquad (34)$$

with

$$\tilde{\Delta}_{j+1/2} = \text{minmod}\,(\Delta_{j+1/2}, b\,\Delta_{j-1/2})$$
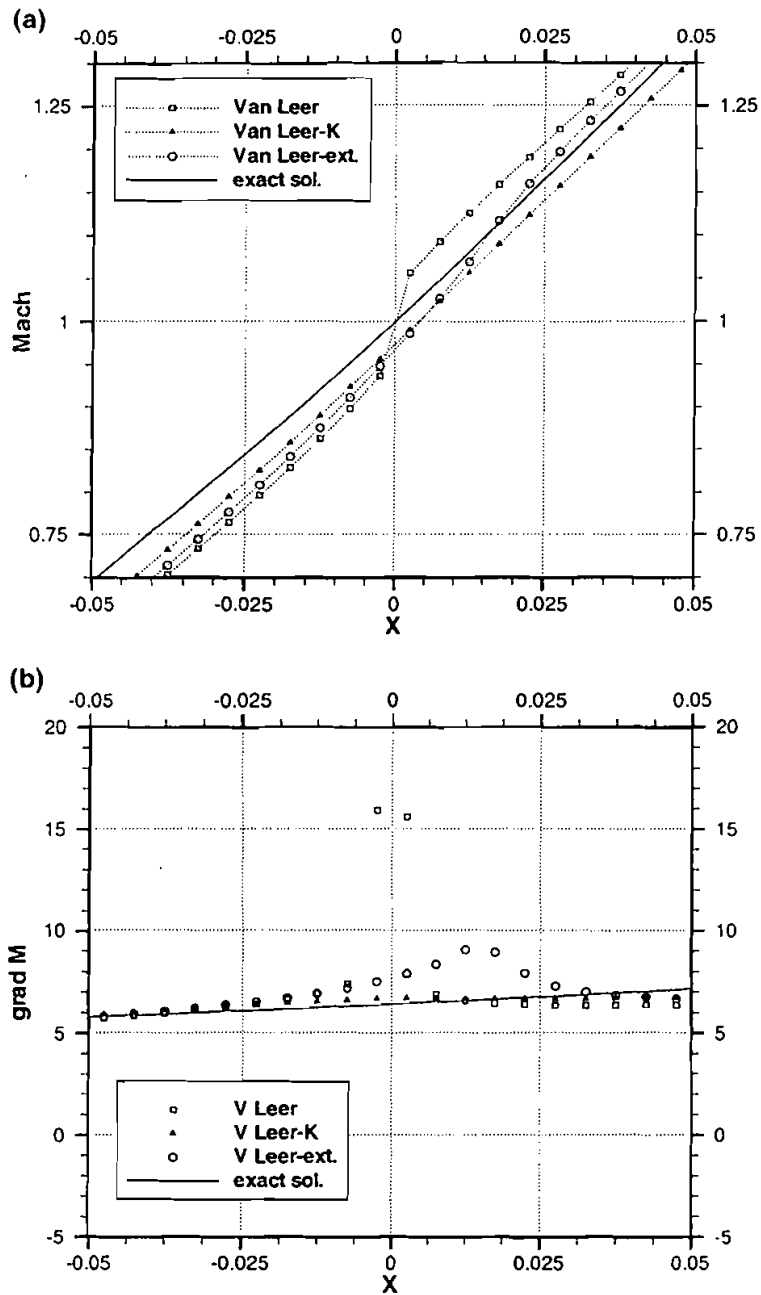$$\tilde{\Delta}_{j+1/2} = \text{minmod}\,(\Delta_{j+1/2}, b\,\Delta_{j+3/2}) \qquad (35)$$

FIGURE 6 Effect of partial upwinding using different pressure correction terms in Van Leer's first order flux: (a) kinetic pressure correction term, (b) extended Van Leer's pressure function.

and

$$\Delta_{j+1/2} = W_{j+1} - W_j \qquad (36)$$

In the present calculations, the compression parameter b has been set to 1. The resulting second

order method has been applied to the transonic expansion problem on a grid which contains 400, 800 and 1600 points (Fig. 8). Compared to a first order result, the second order method leads to a reduced gap around the sonic point. This gap can
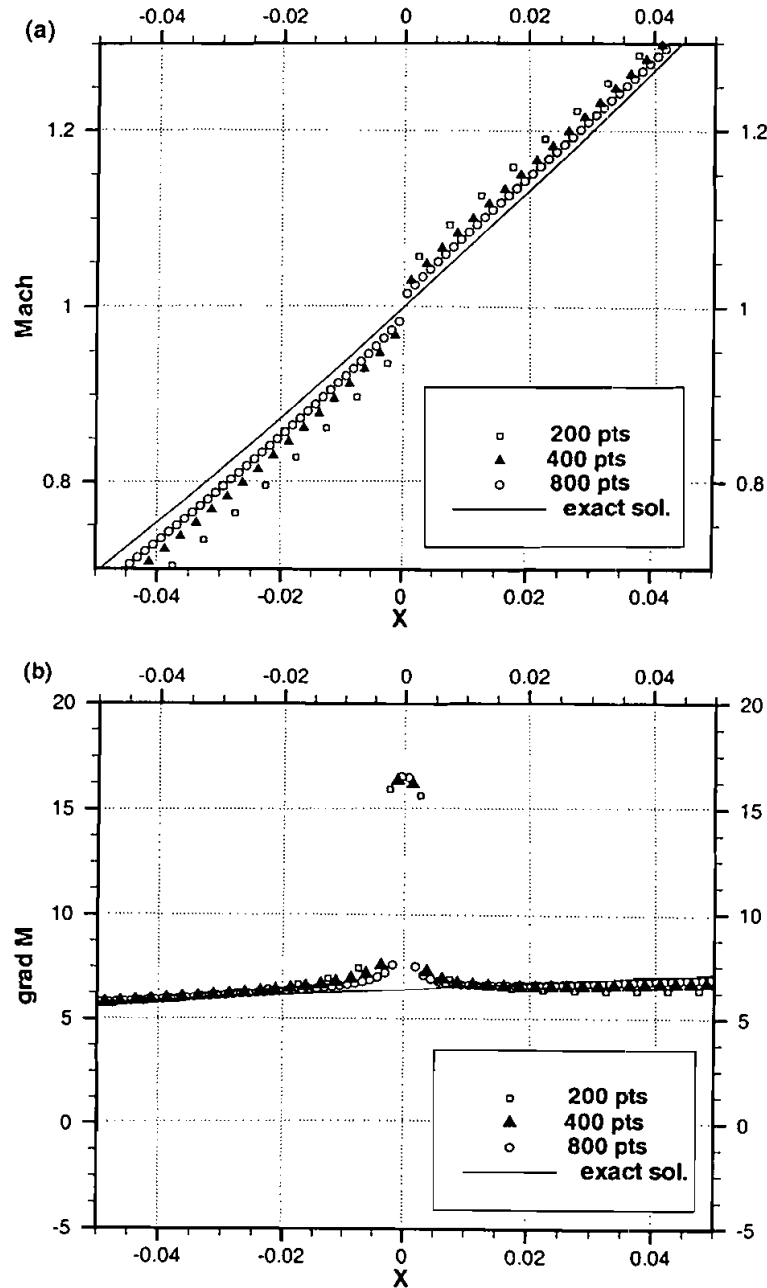
FIGURE 7   Effect of grid resolution for the transonic expansion problem using Van Leer first order method: (a) computed Mach numbers *vs.* exact solution. (b) computed Mach number gradient *vs.* exact solution.

be further decreased by increasing the grid resolution. However, the surprising result is that the gap does not decrease as $O(h^2)$ but only at best as an optimistic $O(h)$. This is confirmed by plotting the Mach number gradient using different grid resolutions (Fig. 9). Figure 9 confirms that increasing the grid resolution does not remove the spurious gradient across the sonic line. On the contrary, it even tends to locally grow around the sonic point, as opposed to first order results
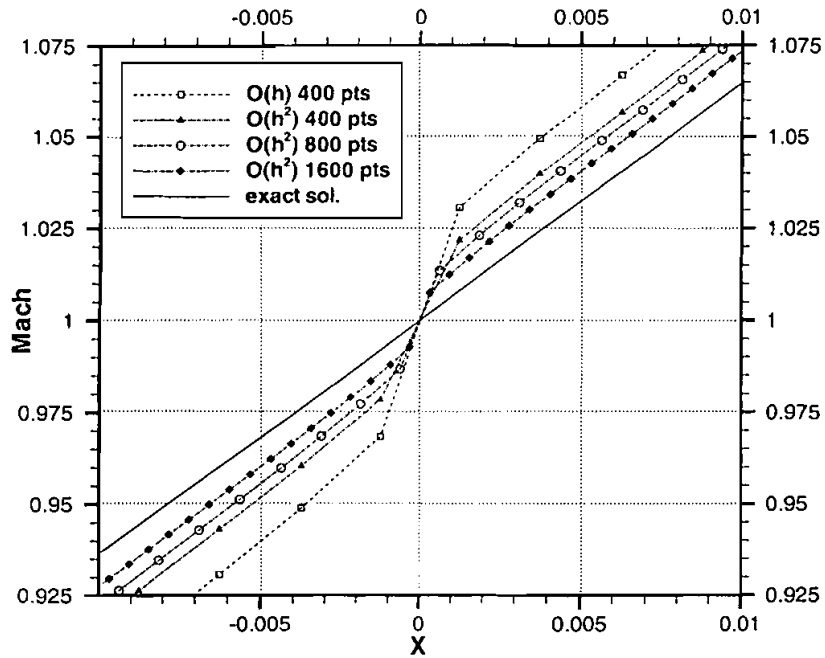
FIGURE 8   Effect of high order resolution for the transonic expansion problem using Van Leer's method: first and second order scheme.
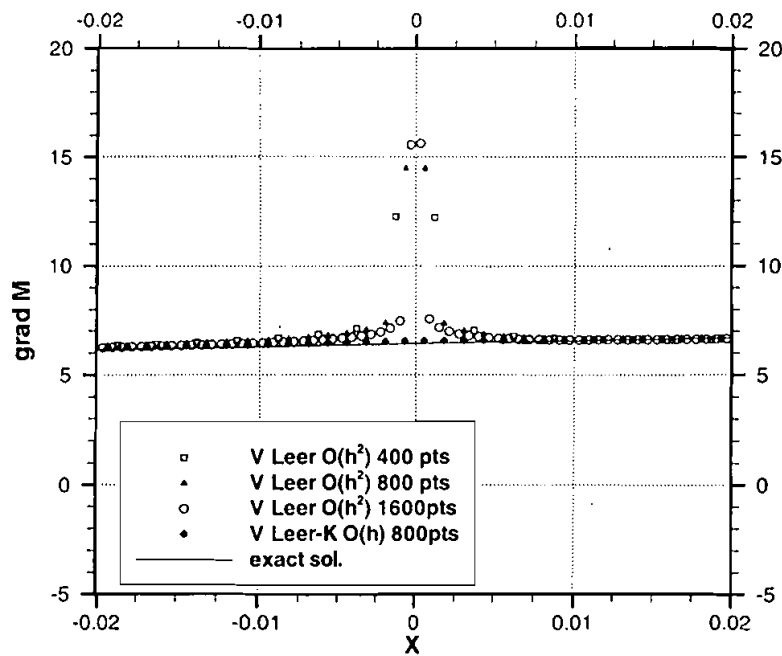

FIGURE 9   Effect of grid resolution on the computed Mach number gradient using Van Leer second order method; comparison with Van Leer-K.

obtained using the proposed pressure correction term which perfectly agree to the exact solution. It should be noticed that the second-order reconstruction makes use of neighboring points which may be located on either sides of the sonic line. Therefore, the reconstruction process leads to a scheme which is not fully upwind since, owing to the presence of the slope limiter, some downstream influence is allowed throughout the sonic line. However, we have no explanation regarding the fact that the glitch amplitude across the sonic point does not locally decrease with the same order of accuracy as the theoretical one.

To conclude on test case (2), one can observe that although the numerical solution does approach the exact solution when the grid resolution is increased, gradients of computed quantities dramatically failed to converge toward the correct solution if an appropriate pressure correction term is not applied, regardless of the high-order extension. This might have some consequences onto the computations of high-temperature gas flows including active chemistry. In these cases, gradients of the computed solution may trigger spurious chemical reactions because stiff source terms are present.

3.3. Test Case (3)

In order to illustrate that the sonic point glitch problem is not limited to one-dimensional configuration, a two-dimensional inviscid unsteady problem is now considered. This problem consists of the diffraction of a traveling shock wave around a diamond shape (see Fig. 10) which lateral sides make an angle of 45 deg. with the horizontal axis, while the tip angle equals 90 deg. The shock wave Mach number M_s is defined as $M_s = U_s/a_s = 2.85$ where U_s is the shock wave speed and a_s is the sound speed of the flowfield at rest. The computational domain is shown on Figure 10 where only every 4 points are represented for clarity. The actual grid size is 200×200. Numerical results at $t = 16$ obtained with AUSM and AUSMK respectively are presented on Figure 11 in terms of pressure contours with a magnified view around the tip of the diamond to better appreciate the effect of the present modification on the unphysical
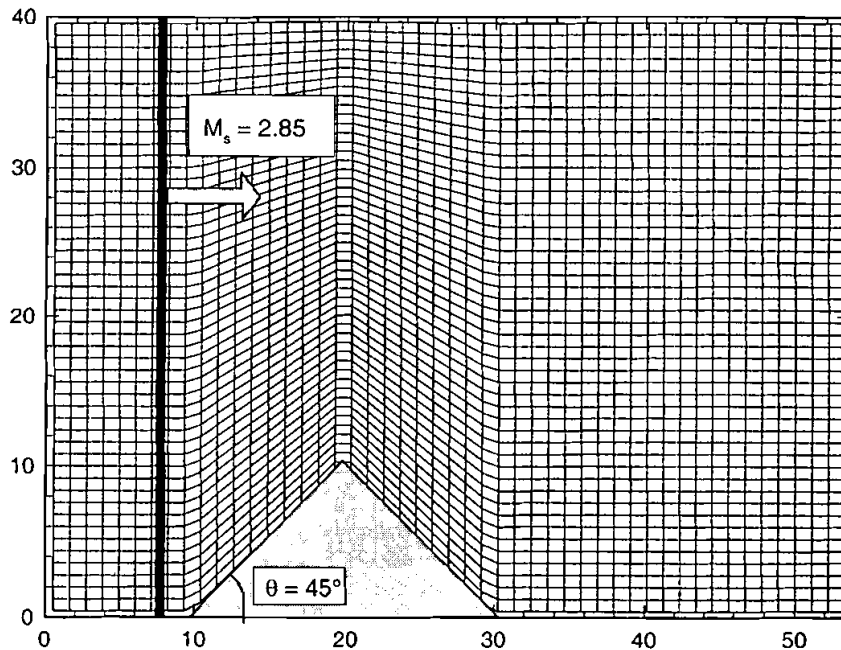

FIGURE 10   Computational domain for the diffracting shock problem.

Pressure contours

1 < p/p0 < 25 - Delta = 1.

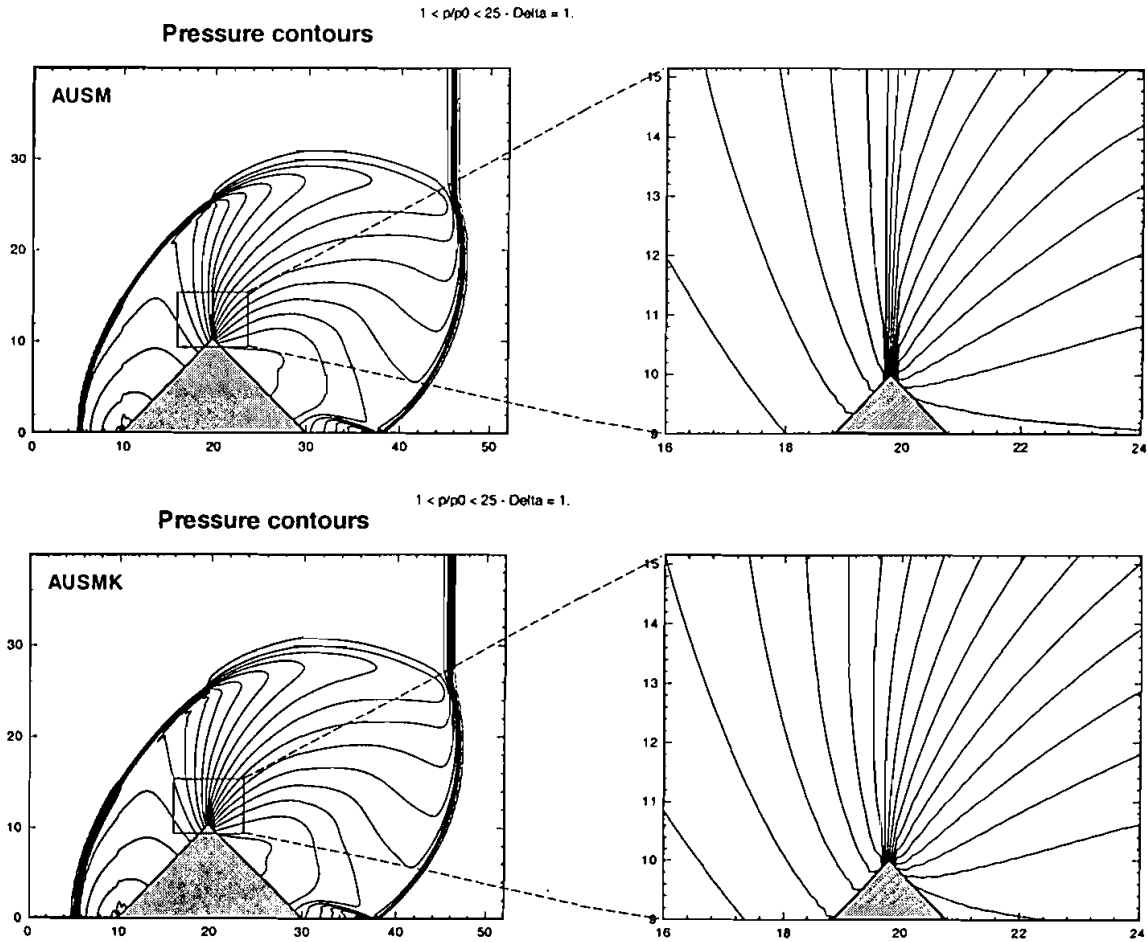

Pressure contours

1 < p/p0 < 25 - Delta = 1.

FIGURE 11 Pressure contours for the diffracting shock problem—Numerical results with AUSM scheme and the modified AUSMK scheme.

discontinuity within the expansion fan. Close analysis reveals that the clustering of iso-pressure lines occurs in the vicinity of the sonic line. Two observations can be made from Figure 11: one is that the spurious clustering of contours has completely vanished when using the KPC term. The second observation is that the KPC term has not significantly affected the solution elsewhere except for the shock thickness ahead of the triangle obstacle which has been slightly broadened.

3.4. Test Case (4)

As a final test case, the shock diffraction around a 90 deg. corner is computed. The advantage of this test case is that the grid is now Cartesian and

uniform with 400 grid points in each direction. Therefore, there is no possible influence of the grid skewness on the sonic line problem. This problem consists of the diffraction of a traveling shock wave of Mach number $M_s = 5.09$ into a domain where the gas is initially at rest. The computational domain consists of a square which sides are 1.0 grid unit-long and whose lower left-hand corner is located at $(-0.1, -0.5)$. The corner is located at the origin of the coordinates system. Post-shock boundary conditions are imposed along the left-hand boundary and first order extrapolation of the conservative variables is applied to the upper, lower and right-hand boundaries. Wall boundary conditions are implemented along the corner sides. Figure 12 shows a side-by-side comparison
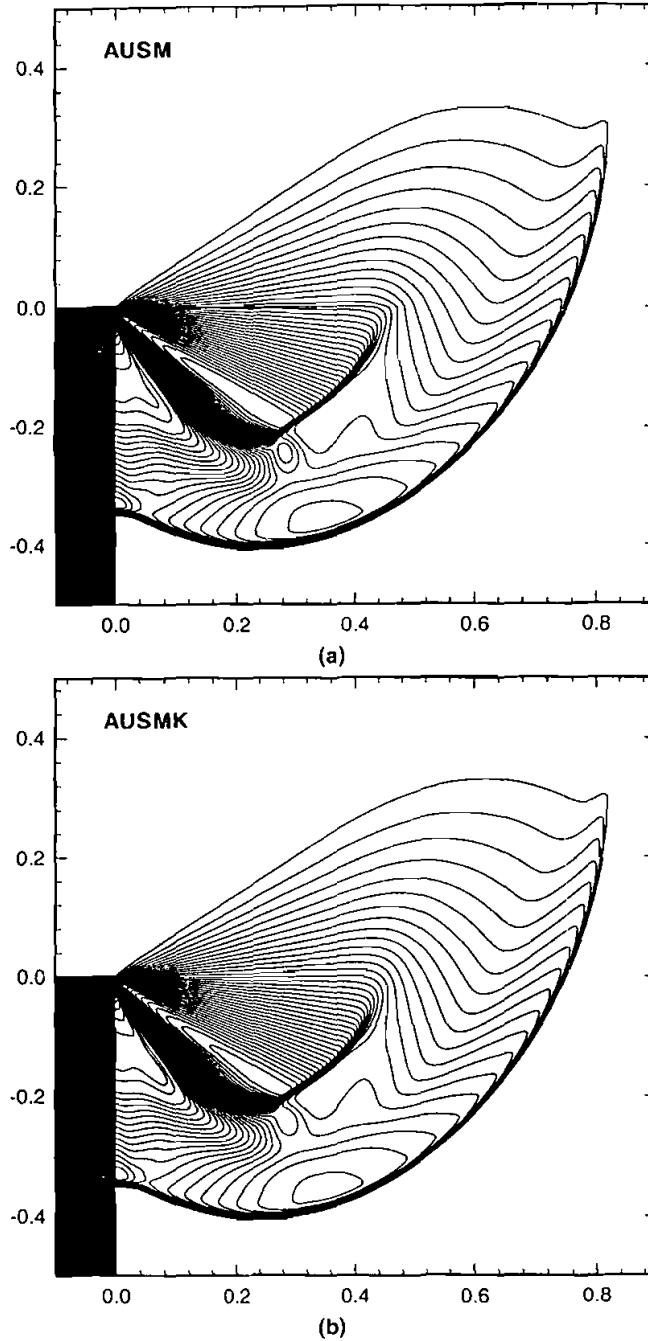
FIGURE 12   Vertical Mach number contours for a $M_x = 5.09$ corner expansion – Numerical results with AUSM scheme (a) and the modified AUSMK scheme (b).

of numerical results obtained with AUSM (Fig. 12(a)) and AUSMK (Fig. 12(b)). Results are shown in terms of contours of vertically projected

Mach numbers M_y defined as
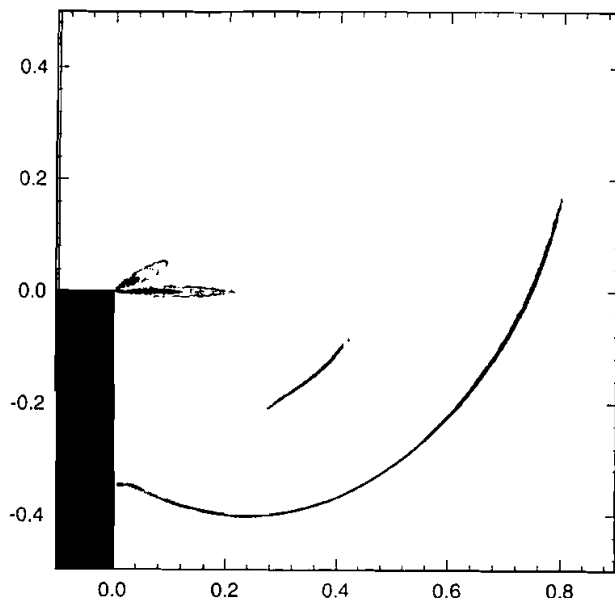
$$M_y = |v|/a \qquad (37)$$

FIGURE 13   Kinetic pressure correction contours for a M_s = 5.09 corner expansion – AUSMK method.

where v is the vertical component of the velocity and a is the local sound speed value. This quantity is useful here since it allows to understand that in two-dimensional flows, the sonic line glitch occurs whenever the normal projection of the Mach number with respect to the interface reaches 1.0. As observed in the previous test case, it appears that the "sonic line" problem has completely vanished when using the KPC term. Moreover, in order to check that the added pressure term becomes active only in restricted areas, a contour of the vertical component of the pressure correction ΔF is shown on Figure 13. It is noticeable that the kinetic pressure correction essentially affects the region where the isolines tend to focus. As expected, because of its formal dependency on pressure levels, it also reaches significant values in the shock profile but to a lower degree.

4. CONCLUSIONS

A simple and straightforward modification of various numerical flux functions which removes the sonic point glitch problem produced by almost

all current numerical algorithms has been proposed. By using an upwind infinitely differentiable (UID) flux function, it is demonstrated that the flaw does not come from an insufficient smoothness of the flux functions but is dependent upon some specific properties of kinetic schemes in which the full upwinding of the numerical flux is not enforced when the flow is locally supersonic. One-dimensional and two-dimensional compressible Euler flow problems have been selected in which the sonic point glitch problem is clearly visible. In all encountered situations, the KPC term has been found to cure the unphysical focusing of iso-lines in regions where the normal Mach number is close to unity without affecting the rest of the computed solution. The KPC term can be easily added to any flux function, ranging from every FVS method to all FDS and hybrid methods such as AUSM. The addition of the KPC term only slightly increases the shock thickness in some cases and simultaneously maintains the exact resolution of steady contact discontinuities if this property was already satisfied by the original scheme. As an example, AUSM method, for which the kinetic pressure correction comes

naturally, results in an improved version called AUSMK which proved to be very helpful for the computation of unsteady compressible flow problems where discontinuous initial conditions are used and for all compressible flow problems in which a geometrical singularity is present. Finally, this study has revealed that full upwinding of the numerical flux functions may not be a desirable property to construct future upwind methods.

References

Chattot, J.-J. (1998) "A Conservative Box-Scheme for the Euler Equations", *Int. J. of Numer. Meth. in Fluid*, to appear.

Coquel, F. and Liou, M. S. (1992) "Stable and Low Diffusive Hybrid Upwind Splitting Methods", In: *Computational Fluid Dynamics '92*, 1, Elsevier Science Publ., pp. 9–16.

Godunov, S. K. (1959) "A Finite Difference Method for the Numerical Computation of Discontinuous Solutions of the Equations of Fluid Dynamics", *Math. Sbornik*, 47, 271–290. Translated as U.S. Dept. of Commerce JPRS 7225, 1960.

Hänel, D., Schwane, R. and Seider, G. (1987) "On the Accuracy of Upwind Schemes for the Solution of the Navier–Stokes Equations", *AIAA Paper 87-1105-CP*.

Harten, A. and Hyman, J. M. (1983) "Self-Adjusting Grid Methods for One-Dimensional Hyperbolic Conservation Laws", *J. Comput. Phys.*, 43, 357–372.

Liou, M. S. and Steffen, C. J. (1993) "A New Flux-Splitting Scheme", *J. Comput. Phys.*, 107, 23–39.

Moschetta, J. M. and Pullin, D. I. (1997) "A Robust Low Diffusive Kinetic Scheme for the Navier–Stokes/Euler Equations", *J. Comput. Phys.*, 133, 193–204.

Osher, S. and Solomon, F. (1982) "Upwind Difference Schemes for Hyperbolic Systems of Conservation Laws", *Math. of Comput.*, 38, 339–374.

Pullin, D. I. (1980) "Direct Simulation Methods for Compressible Inviscid Ideal-Gas Flow", *J. Comput. Phys.*, 38, 231–244.

Roe, P. L. (1981) "Approximate Riemann Solvers, Parameter Vectors, and Difference Schemes", *J. Comput. Phys.*, 43, 357–372.

Steger, J. L. and Warming, R. F. (1981) "Flux Vector Splitting for the Inviscid Gas-dynamics Equations with Applications for Finite Difference Methods", *J. Comput. Phys.*, 40, 263–293.

Van Leer, B. (1982) "Flux Vector Splitting for the Euler Equations", In: *Proc. 8th Int. Conf. Num. Meth. Fluid Dyn.*, Lecture Notes in Physics. Springer Verlag, pp. 507–512.

Xu, K., Martinelli, L. and Jameson, A. (1995) "Gas-Kinetic Finite Volume Methods. Flux-Vector Splitting and Artificial Diffusion", *J. Comput. Phys.*, 120, 48–65.